Generalized Regression Neural Network and Empirical Models to Predict the Strength of Gypsum Pastes Containing Fly Ash and Blast Furnace Slag

Tahir Kemal Erdem[1] · Okan Cengiz[2] · Gökmen Tayfur[1]

Abstract

Gypsum is widely used in constructions owing to its easy application, zero shrinkage, and excellent fire resistance. Several parameters can affect the properties of gypsum pastes. To study the strength of the gypsum pastes experimentally by trying all these parameters is time-consuming and costly. Therefore, artificial intelligence methods can be very useful to predict the paste strength, which, in turn, can reduce the number of trial batches. Based on experimental data, the generalized regression neural network (GRNN) and empirical models were developed to predict strength of gypsum pastes containing fly ash (FA) and blast furnace slag (BFS). Gypsum content, pozzolan content, curing temperature, curing duration, and testing age constituted the input variables of the models while the paste strength was the target output. The trained and tested GRNN model was found to be successful in predicting strength. Sensitivity analysis by the GRNN model revealed that the curing duration and temperature were important sensitive parameters. In addition to the GRNN model, empirical models were proposed for the strength prediction. The same input variables formed the input vectors of the empirical models. The same dataset used for the calibration of the GRNN model was employed to establish the empirical models by employing genetic algorithm (GA) method. The empirical models were successfully validated. The GRNN and GA_based empirical models were also tested against the multi-linear regression (MLR) and multi-nonlinear regression (MNLR) models. The results showed the outperformance of the GRNN and the GA_based empirical models over the others.

Keywords GRNN · Empirical model · Genetic algorithm (GA) · Gypsum paste strength · Fly ash · Blast furnace slag · MLR · MNLR

1 Introduction

Gypsum, which has been used as a binder for several centuries, is an important construction material. It is produced from natural gypsum rock which is available all over the world. Global crude gypsum production in 2015 was estimated to be 261 Mt. China was the leading producer of crude gypsum in 2015 with an estimated 130 Mt, followed, in decreasing order by tonnage, by Iran with 16.0 Mt, the USA with 15.2 Mt and Turkey with 12.6 Mt [1]. The natural gypsum rock reserve only in Beypazarı, a district in Turkey, is estimated to be above 1 billion tons [2, 3].

When the natural gypsum rock ($CaSO_4 \cdot 2H_2O$ or calcium sulfate dihydrate) is heated, either partial or complete dehydration occurs depending on the temperature, and different products are obtained accordingly. Hemihydrate gypsum is formed when the natural gypsum rock is heated at temperatures between 100 C and 190 C and anhydrite is formed when the heating temperature is above 190 °C. When mixed with water, both of these products initially form a plastic paste, and then gain rigidity and strength in time by making a network of gypsum crystals.

Gypsum is used especially in hemihydrate form in buildings, ceramics, and medical industries. In building construction, hemihydrate gypsum paste is a popular finishing

✉ Tahir Kemal Erdem
    tahirkemalerdem@iyte.edu.tr

    Okan Cengiz
    okan.cengiz@tubitak.gov.tr

    Gökmen Tayfur
    gokmentayfur@iyte.edu.tr

1   Department of Civil Engineering, İzmir Institute of
    Technology, Urla, Izmir 35430, Turkey

2   The Scientific and Technological Research Council of
    Turkey, Ankara, Turkey

material due to its excellent performance, attractive appearance, easy application, its healthful contribution to living, zero shrinkage, and excellent fire resistance [4, 5]. Despite these advantages, its use may be hindered for some applications due to its relatively higher porosity, low water resistance, and low strength. Therefore, several additives such epoxy resins, polymers, slags, waterproofing materials, and fly ash can be used to overcome such disadvantages [6–8]. Moreover, water-to-binder ratio, curing age, curing temperature, and age are some of the other parameters that can affect the properties of gypsum pastes. To improve the strength of the gypsum pastes, trying all these parameters in an experimental study requires long time, much manpower, and high quantity of materials, resulting in a higher cost of the product. Therefore, artificial intelligence methods can be very useful to predict the paste strength, which helps to reduce the number of trial batches.

There are several studies in the literature that use regression or artificial intelligence methods to predict the strength of the concretes from a sort of input parameters [9–14]. On the other hand, there are only a few studies involving gypsum and artificial intelligence. Oktay and Odabaş [15] successfully predicted the properties of plasters containing phosphogypsum (a type of artificial gypsum) and perlite by using artificial neural network (ANN) and regression models. The study of Yılmaz and Yüksek [16] was about predicting the strength and elasticity modulus of gypsum rock by regression, ANN, and ANFIS models. However, to the best knowledge of the authors, no research paper has been published on predicting the strength of gypsum pastes by regression, empirical, or artificial intelligence methods.

The objective of this study is twofold: (1) to apply the generalized regression neural network (GRNN) to predict strength of gypsum pastes and (2) to develop empirical models for the same predictive purpose. The development of the models was carried out by considering, in the input vector, datasets within a wide range of Gypsum content ($G\%$), Pozzolan content (FA% or BFS%), curing Temperature (T), curing duration (D), and testing age (Age). This is the first study, as far as the authors know, that develops empirical models for the gypsum paste strength. The GA which is robust and is not constraint by the differentiability and/or integrability of the objective function [17] is employed to find the optimal values of the coefficients and exponents of the empirical models (GA_based empirical models). Also, this study is the first that applies the GRNN for the gypsum paste strength predictions. GRNN is one of the training algorithms of artificial neural networks. Although the backpropagation training algorithm in the feed-forward neural networks (FFNN) is quite common in engineering applications [17], the network can be sometimes trapped by the local error minima and it can sometimes generate estimates that are not physically plausible [18]. The performance of the GRNN

and GA_based empirical models was also tested against those of the MLR and MNLR modes.

This study develops GRNN and empirical models to predict gypsum paste strength. In addition to the fact that such methods are the first time developed in this study to predict gypsum paste strength, they can also save time, labor, and money by reducing the experimental trial batches.

2 Data

As stated previously, the data were taken from a study of Cengiz [8] in which gypsum pastes were prepared by using gypsum hemihydrate and various amounts pozzolans (FA or BFS). The weight of the pozzolan was 15, 30, 45, 60, and 75% of the gypsum + pozzolan mixture. To enable pozzolanic reactions, hydrated lime was also used and its amount was always 40% of the pozzolan weight. For example, a gypsum + pozzolan mixture containing 15% pozzolanic material consisted of 85 units gypsum and 15 units pozzolanic material. Such mixtures contained $15 \times 40\% = 6$ units lime, as well. Therefore, by considering the total weight of the binder as 100 units, the mix actually contains 80.19% gypsum, 14.15% pozzolanic material, and 5.66% lime by weight. The gypsum and pozzolan contents of the mixtures used in that study can be seen in Table 1. The water-to-binder ratio was constant at 0.60 in all mixtures. The fresh pastes were molded into the 5-cm cubes and stored in their molds at 20 °C for 24 h. Afterward, the 1-day specimens were cured in an oven at 50 °C or 80 °C for 4, 12, 24, or 72 h. At the end of the curing period, they were kept in water at 20 °C until their testing days. Compressive strength of the mixtures was determined at 7, 14, and 28 days. Since the main focus of this paper is on artificial intelligence methods, the details of the experimental work were left to the original study [8].

According to the experimental program summarized above, the input parameters and their corresponding values used for the models constructed in this study are given in Table 1.

As given in Table 1, for each pozzolan type, there were 5 (types of mixtures) × 2 (values of curing temperature) × 4 (values of curing duration) = 40 specimen types. For each specimen type, there were 3 compressive strength values corresponding to 7, 14 and 28 days. Therefore, totally 120 datasets were established for each pozzolan type; 72 out of these 120 datasets were used to train (calibrate) the models while the rest (48 datasets) were used to test (validate) the models. In other words, 60% of the data were taken as training (calibration) data and the 40% of the data were taken as testing (validation) data. The classification of the data was made randomly.

Table 1 The input parameters and their corresponding values

Gypsum content in percent ($G\%$)	Pozzolan (FA or BFS) content in percent (FA% or BFS%)	Curing temperature in °C (T)	Curing duration in hours (D)	Testing age in days (age)
80.19	14.15	50, 80	4, 12, 24, 72	7, 14, 28
62.50	26.79	50, 80	4, 12, 24, 72	7, 14, 28
46.61	38.14	50, 80	4, 12, 24, 72	7, 14, 28
32.26	48.39	50, 80	4, 12, 24, 72	7, 14, 28
19.23	57.69	50, 80	4, 12, 24, 72	7, 14, 28

Fig. 1 Schematic representation of GRNN model
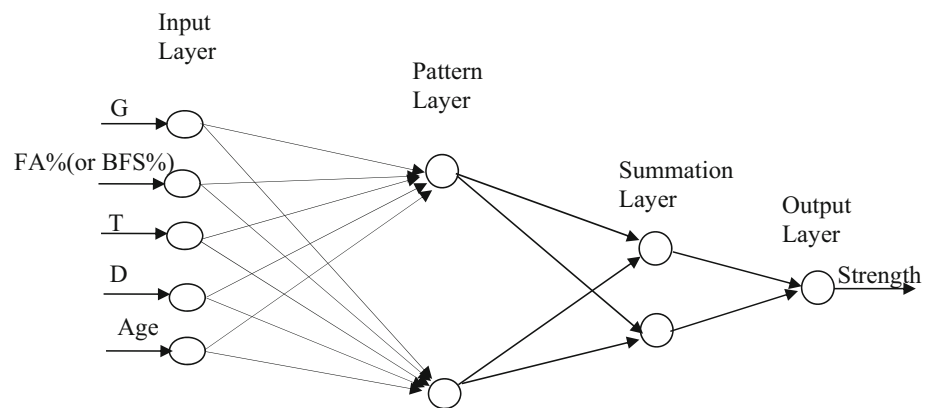
3 Models

3.1 Generalized Regression Neural Network (GRNN)

The GRNN structure has four layers (Fig. 1) of input, pattern, summation, and output [19]. The number of input units in the first layer is equal to the total number of input variables, and these, in this study, are gypsum content ($G\%$), pozzolan content (FA% or BFS%), curing temperature (T), curing duration (D), and testing age (Age). The second layer has the pattern units whose outputs are passed on to the summation units in the third layer. The summation layer has two units of the S-summation neuron and the D-summation neuron where the S-summation neuron computes the sum of the weighted outputs of the pattern layer while the D-summation neuron does the same for the non-weighted outputs. The connection weights are set unity between the pattern layer neurons and the D-summation neuron [20]. The output layer divides the output of each S-summation neuron by that of each D-summation neuron, yielding the predicted value to an unknown vector, which is the strength (S) in this study.

The mathematical background of the algorithm is quite different than that of the back-propagation algorithm of FFNN [17]. The GRNN approximates any arbitrary function between input and output vectors, drawing the function estimate directly from the training data. When provided with the training datasets of x and y variables, the method estimates a joint probability density function (pdf) of x and y as given in Eq. 1:

$$E[y|x] = \frac{\int_{-\infty}^{\infty} y f(x, y) \mathrm{d}y}{\int_{-\infty}^{\infty} f(x, y) \mathrm{d}y} \tag{1}$$

$f(x,y)$ is usually estimated from a sample of the observations of the variables (x, y) as follows:

$$\hat{f}(x, y) = \frac{1}{(2\pi)^{(p+1)/2} \sigma^{(p+1)}} \frac{1}{n} \sum_{i=1}^{n}$$
$$\exp\left[-\frac{(x - x_i)^T (x - x_i)}{2\sigma^2}\right] \exp\left[-\frac{(y - y_i)^2}{2\sigma^2}\right] \tag{2}$$

where $\hat{f}(x, y)$ is the probability estimator; n is the number observation; σ is smoothing parameter; and p is the dimension of the vector variable x. If we define the scalar function d_i as

$d_i^2 = (x - x_i)^T (x - x_i)$ and substitute it into Eq. 2 and perform the indicated summations in Eq. 2, then we can obtain the estimate of output variable, y as follows:

Fig. 2 Example for crossover and mutation operations

Parent	1	0	1	1	1	0	1	1	→	187
Parent	1	1	1	0	1	0	0	0	→	232

after cross-over

Offspring-I	**1**	**1**	**1**	**0**	1	0	0	1	→	233
Offspring-II	**1**	**0**	**1**	**1**	1	0	1	0	→	186

after mutation

New offspring-I	**1**	**0**	1	**0**	1	0	0	1	→	169
New offspring-II	**1**	**1**	**1**	**1**	1	0	1	0	→	250

$$\hat{y}(x) = \frac{\sum_{i=1}^{n} y_i \exp\left(-\frac{d_i^2}{2\sigma^2}\right)}{\sum_{i=1}^{n} \exp\left(-\frac{d_i^2}{2\sigma^2}\right)} \tag{3}$$

The only parameter which is adjusted in GRNN is the smoothing parameter, σ, and its optimal value can often be determined experimentally [20]. Further details on GRNN can be found elsewhere [17, 18, 21, 22].

Peng and Dai [23] reviewed some papers published in the last two decades on an interesting soft computing method (Neutrosophic Set) that can be used to characterize the uncertain information more sufficiently and accurately than intuitionistic fuzzy set. They also developed new approaches for the multi-attribute decision-making (MADM) method under single-valued neutrosophic environment [24].

It is also possible to see newly developed artificial intelligence algorithms such as the neural network ensemble approach (NNEA) [25], the neural network-based linear ensemble framework (NNLEF) [26], the adaptive differential evolution-based back-propagation neural network (ADE-BPNN) [27], and the differential evolution algorithm (DEA) [28].

3.2 Genetic Algorithm (GA)

GA concept is based on the fittest of survival and the Mendelian genetics. As such, it employs the operations of selection and elimination, working with the strong individuals (chromosomes), each of which is a candidate for a solution. It employs the genetic operations of crossovering and mutation for the chromosomes, each of which consists

of genes. Note that each gene consists of bits of 0 and 1, and each gene is a model parameter. On the other hand, each chromosome consists of the total number of genes of the process. The fitness of a chromosome, $F(C_i)$, can be found as:

$$F(C_i) = \frac{f(C_i)}{\sum_{i=1}^{N} f(C_i)} \tag{4}$$

where N is the total number of chromosomes, C_i is the ith chromosome, $f(C_i)$ is the functional value of the ith chromosome, and $F(C_i)$ the fitness value of the ith chromosome.

After calculating the fitness of each chromosome, the selection process is performed using either the roulette wheel or the ranking method. After the selection process, crossover and mutation operations are performed to produce new generations (chromosomes). Figure 2 is an example for the crossover and mutation operations. As seen, the genes of the first two chromosomes (parent chromosome I and parent chromosome II) were cut from the fourth digit on the left and interchanged. This resulted in a new pair of chromosomes (offspring I and offspring II). The original values 187 and 232 became 233 and 186, respectively. The mutation operation was applied onto the second digit from the left of each offspring by simply reversing digit 1–0 and digit 0–1, respectively. After the mutation operation, 233 and 186 became 169 and 250, respectively. One can find more details on GA in [17, 29, 30].

The flowchart showing the relations among the data, GRNN, and GA models and the testing of these models against the MLR and MNLR methods (given in Sect. 4.3) is represented in Fig. 3.

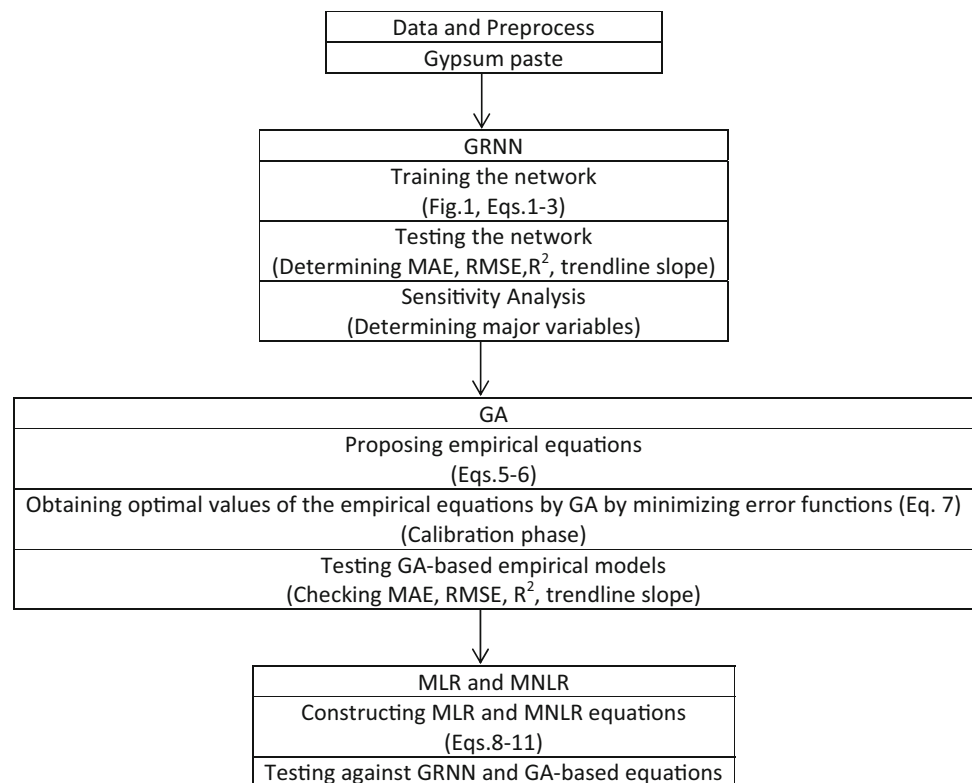**Fig. 3** Flowchart showing the relationship of the used technologies

| Data and Preprocess |
| Gypsum paste |

↓

| GRNN |
| Training the network (Fig.1, Eqs.1-3) |
| Testing the network (Determining MAE, RMSE, R^2, trendline slope) |
| Sensitivity Analysis (Determining major variables) |

↓

| GA |
| Proposing empirical equations (Eqs.5-6) |
| Obtaining optimal values of the empirical equations by GA by minimizing error functions (Eq. 7) (Calibration phase) |
| Testing GA-based empirical models (Checking MAE, RMSE, R^2, trendline slope) |

↓

| MLR and MNLR |
| Constructing MLR and MNLR equations (Eqs.8-11) |
| Testing against GRNN and GA-based equations |

Table 2 Performance of different methods for the FA pastes

	Calibration (training)				Validation (testing)			
	MLR	MNLR	GA	GRNN	MLR	MNLR	GA	GRNN
MAE (MPa)	0.673	0.661	0.403	0.027	0.680	0.663	0.366	0.336
RMSE (MPa)	0.885	0.876	0.569	0.063	1.050	1.031	0.547	0.585
R^2	0.779	0.784	0.911	0.999	0.773	0.782	0.951	0.926
Trendline slope	0.779	0.783	0.871	0.995	0.658	0.671	0.824	0.890

4 Model Applications

4.1 GRNN Model Application

As presented in Fig. 1, gypsum content ($G\%$), pozzolan content (FA% or BFS%), curing temperature (T), curing duration (D), and testing age (Age) constituted the input variables while the strength is the output variable. Seventy-two datasets were used for the training of the network while the remaining 48 sets were used for testing. The training is carried out while minimizing the mean absolute error (MAE), the root-mean-square error (RMSE) and maximizing the R^2 values. The smoothing parameter, σ, is adjusted as 1.14. In this study, NeuroTools, the package program of Palisade Corporation [31] was employed.

As seen in Table 2, the training of GRNN was successfully accomplished with MAE = 0.027 MPa, RMSE = 0.063 MPa, and $R^2 = 0.999$ for the FA pastes. Figure 4 presents measured versus GRNN-predicted strength values for the FA pastes.

As seen, the model made good predictions with MAE = 0.336 MPa, RMSE = 0.585 MPa, and $R^2 = 0.93$ (see Table 2). The slope of the fitting line is almost 0.9, and the intercept is close to zero (see Fig. 4).

In a similar fashion, the GRNN model was trained for BFS pastes with MAE = 0.242 MPa, RMSE = 0.317 MPa, and $R^2 = 0.981$ (Table 3). Figure 5 presents the model performance for the testing stage. The network performed good in predicting measured strength values for the BFS pastes with MAE = 0.458 MPa, RMSE = 0.606 MPa, and $R^2 = 0.93$ (see Table 3). The slope of the fitting line is 0.93, and the intercept is 0.32 (see Fig. 5).

4.2 GA Model Application

The following empirical models, Eqs. 5 and 6, are proposed in this study to predict strength as a function of gypsum content ($G\%$), pozzolan content (FA% or BFS%), curing temperature (T), curing duration (D), and testing age (age) for gypsum
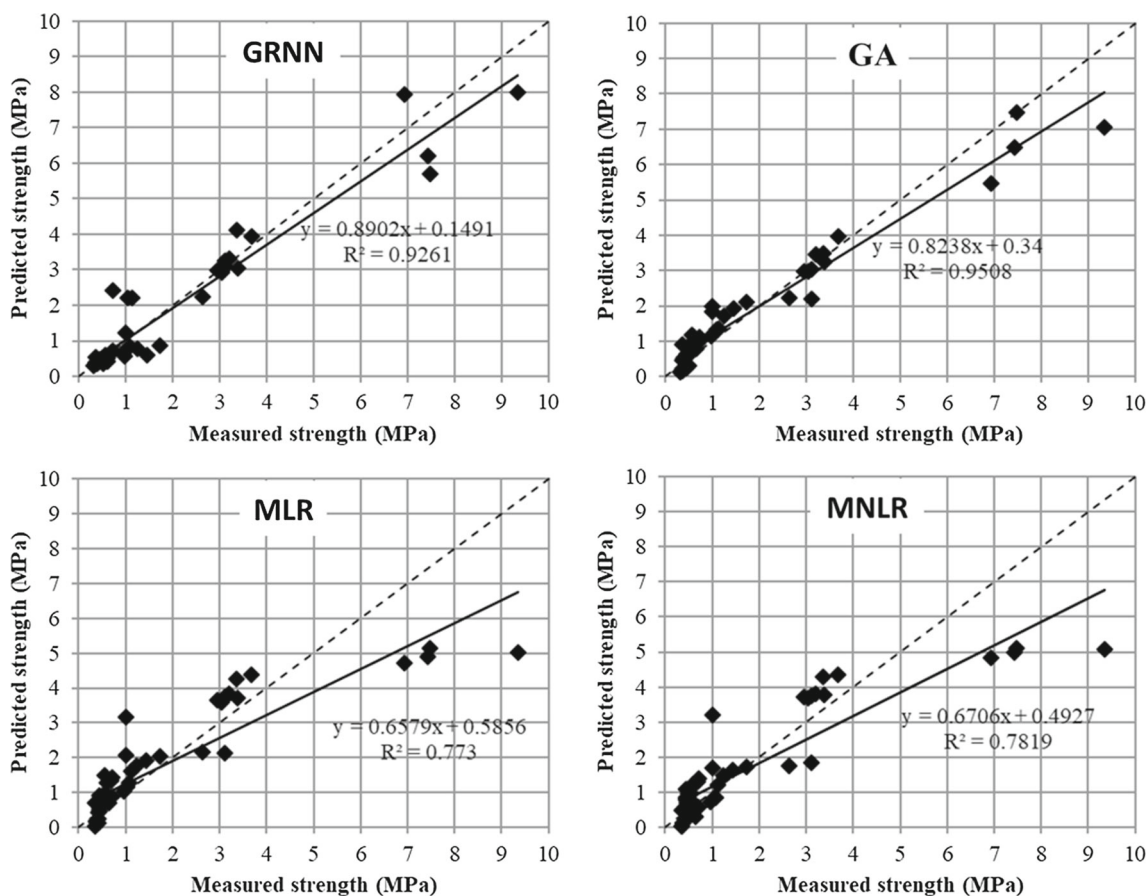
Fig. 4 Prediction results of the models during the validation (testing) stage for FA pastes

Table 3 Performance of different methods for the BFS pastes

	Calibration (training)				Validation (testing)			
	MLR	MNLR	GA	GRNN	MLR	MNLR	GA	GRNN
MAE (MPa)	0.526	0.577	0.534	0.243	0.640	0.635	0.471	0.458
RMSE (MPa)	0.638	0.708	0.656	0.317	0.801	0.768	0.639	0.606
R^2	0.915	0.897	0.911	0.981	0.883	0.888	0.912	0.925
Trendline slope	0.915	0.863	0.909	0.942	1.013	0.961	0.898	0.929

paste containing fly ash (FA) and ground granulated blast furnace slag (BFS), respectively.

$$\text{Strength} = c_1 * (G\%)^a * (FA\%)^b * (T)^c * (D)^d * (\text{Age})^e \tag{5}$$

$$\text{Strength} = c_1 * (G\%)^a * (BFS\%)^b * (T)^c * (D)^d * (\text{Age})^e \tag{6}$$

where c_1, a, b, c, d, and e are the empirical coefficients and strength is in MPa. The optimal values of these coefficients were obtained by employing the GA method which minimizes the mean absolute error (MAE) between the measured

strength and that calculated by the model (Eq. 5 or Eq. 6), as follows:

$$\text{MAE} = \frac{1}{N} \sum_{i=1}^{N} |S_{\text{Model}} - S_{\text{Measured}}| \tag{7}$$

where S_{Model} is the strength computed by the empirical model (Eq. 5 or Eq. 6), S_{Measured} is the measured strength, and N is the number of datasets used in the calibration procedure.

The GA model employed 80 chromosomes, 80% crossover, 4% mutation rate, and 6000 iterations were used in Evolver, the GA package software of Palisade Corporation [31]. The same datasets used for the training of the GRNN were employed for the calibration of Eqs. 5 and 6 by the GA.
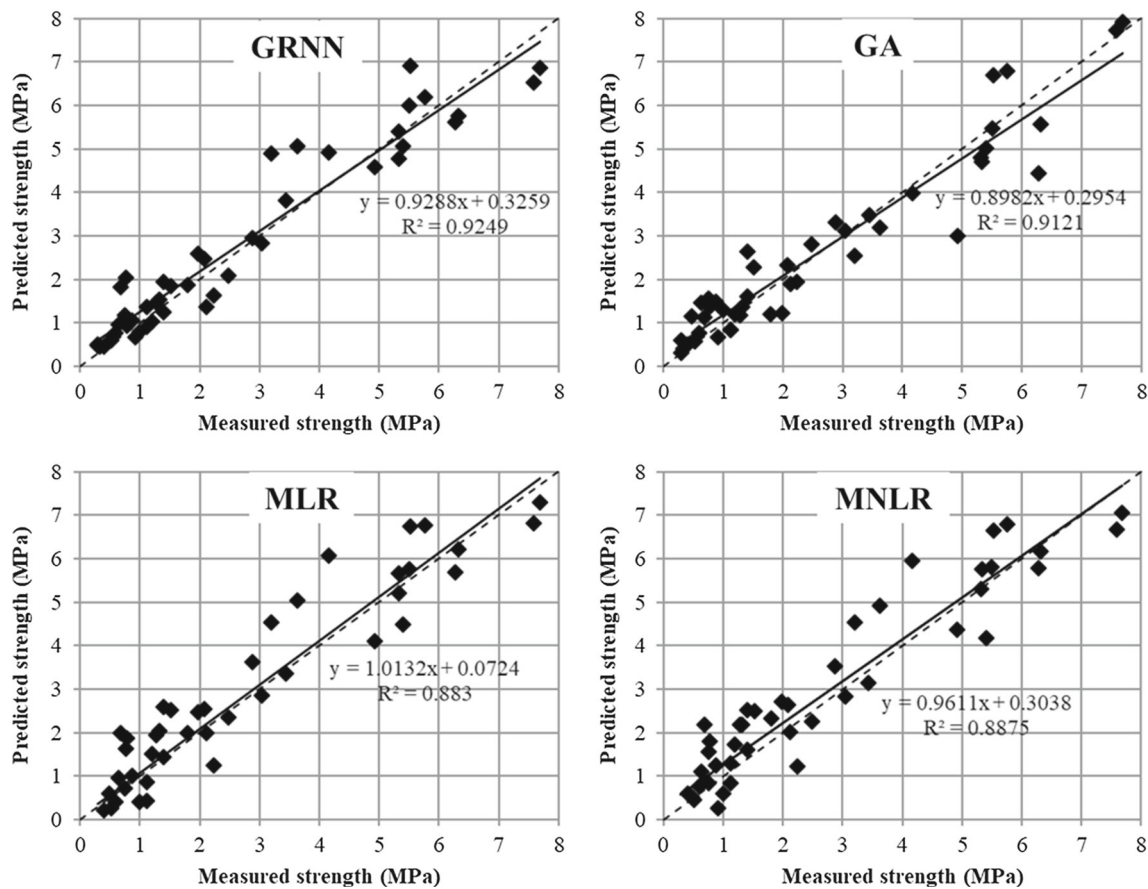
Fig. 5 Prediction results of the models during the validation (testing) stage for BFS pastes

Table 4 Optimal values of the coefficients in Eqs. 5, 8 and 10 for the FA pastes

	c_1	c_2	c_3	c_4	c_5	a	b	c	d	e
MLR	-0.0310	-0.0304	0.0365	0.0578	0.0147	–	–	–	–	–
MNLR	-0.0014	-0.0006	0.0001	0.0041	0.0013	1.5223	1.6589	2.3251	1.6002	1.6146
GA	3×10^{-5}	–	–	–	–	0.0121	0.3738	1.3821	0.9824	0.1820

Table 5 Optimal values of the coefficients in Eqs. 6, 9 and 11 for the BFS pastes

	c_1	c_2	c_3	c_4	c_5	a	b	c	d	e
MLR	-0.0467	-0.0136	0.0361	0.0703	0.0740	–	–	–	–	–
MNLR	-0.0002	4×10^{-5}	2×10^{-5}	0.0153	0.0147	2.0396	2.3786	2.5390	1.3334	1.4144
GA	0.0001	–	–	–	–	0.2592	0.9111	0.7512	0.5985	0.3241

The calibrated (optimal) values of the coefficients are summarized in Table 4 for the FA pastes and in Table 5 for the BFS pastes. The respected error measures are summarized in Tables 2 and 3.

The same testing datasets employed in the GRNN were also used for the validation of Eqs. 5 and 6 whose coefficients (see Tables 4, 5) were optimized by the GA. The validation runs showing the predictions of strengths for the FA and BFS pastes are, respectively, shown in Figs. 4 and 5. As seen, for

both cases, the empirical equations performed well, with low errors and high R^2 values (see Tables 2 and 3).

4.3 Multiple Linear Regression (MLR) and Multiple Nonlinear Regression (MNLR) Equations

In order to compare the performances of the GRNN and the empirical equations (Eqs. 5, 6) (herein they are called GA_based empirical models) to predict strength, MLR and

MNLR equations were also established for the same purpose. MLR models (Eqs. 8, 9) for predicting strength of gypsum pastes containing fly ash and ground granulated blast furnace slag were, respectively, established as follows:

$$
\begin{aligned}
\text{Strength} = {}& c_1 * (G\%) + c_2 * (FA\%) + c_3 * (T) \\
& + c_4 * (D) + c_5 * (\text{Age})
\end{aligned}
\tag{8}
$$

$$
\begin{aligned}
\text{Strength} = {}& c_1 * (G\%) + c_2 * (BFS\%) + c_3 * (T) \\
& + c_4 * (D) + c_5 * (\text{Age})
\end{aligned}
\tag{9}
$$

MNLR models (Eqs. 10 and 11) for predicting strength of gypsum pastes containing fly ash and ground granulated blast furnace slag were, respectively, established as follows:

$$
\begin{aligned}
\text{Strength} = {}& c_1 * (G\%)^a + c_2 * (FA\%)^b + c_3 * (T)^c \\
& + c_4 * (D)^d + c_5 * (\text{Age})^e
\end{aligned}
\tag{10}
$$

$$
\begin{aligned}
\text{Strength} = {}& c_1 * (G\%)^a + c_2 * (BFS\%)^b + c_3 * (T)^c \\
& + c_4 * (D)^d + c_5 * (\text{Age})^e
\end{aligned}
\tag{11}
$$

where c_1, c_2, c_3, c_4, and c_5 are the coefficients and a, b, c, d, and e are the exponents of the regression equations. The same datasets employed for the training of the GRNN and the calibration of the GA_based empirical models (Eqs. 5 and 6) were also used for finding the optimal values of the coefficients and exponents of the regression equations (Eqs. 8–11) (calibration stage). The obtained optimal values of the coefficients and exponents of the regression equations are given in Tables 4 and 5 for the FA pastes and BFS pastes, respectively. Similarly, the MLR and MNLR equations were validated against the same respected sets employed for testing the GRNN and validating the GA_based empirical models. Slope of the linear fitting line on the measured and predicted values, R^2, RMSE, and MAE were calculated for both the calibration and validation stages. The computed error (performance) measures for the calibration and validation stages are presented in Tables 2 and 3 for the FA pastes and BFS pastes, respectively. Figures 4 and 5, respectively, present scatter distribution of the predicted versus measured strength data for the MLR and MNLR equations for the FA and BFS pastes. As seen in Tables 2 and 3, both models showed poor performance with high errors and low R^2 values. The slopes of the fitting lines are around 0.65 which are much lower than 1 and the data distributions around 45° line are much scattered (see Figs. 4, 5).

5 Results and Discussion

The effects of gypsum content, pozzolan type, and curing conditions on the strength of gypsum pastes, which were

discussed in [8], are out of the scope of this study. The paper presented herein focuses on and discusses the use of several methods to predict the strength of gypsum pastes.

Figures 4 and 5 present the prediction results of the models during the testing stage for FA and BFS pastes, respectively. In addition to the linear trendline fitted to the data shown in these figures, the dashed lines are also included to represent the ideal 1:1 relation between measured and predicted data. In order to compare the performance of different methods more precisely, the MAE, RMSE, R^2, and slope of the linear trendline were calculated and are presented in Tables 2 and 3. Moreover, these values for the validation (testing) stage are also represented in Fig. 6 to compare the performance of the used methods.

As seen in Tables 2 and 3, the MLR and MNLR models yielded lower R^2 values and higher error (MAE and RMSE) for both calibration and validation stages when compared to GA_based empirical and GRNN models. As expected, the trendline slopes of GA_based empirical and GRNN models were much closer to 1 when compared to those of MLR and MNLR. This fact and the low performance of MLR and MNLR are apparent from Figs. 4 and 5, as well. Although not shown in these figures, a few of the predictions made by the MLR and MNLR models yielded negative strength values which have no physical meaning. The negative predictions resulted from the negative c_1 coefficients, given in Tables 4 and 5, which belong to the gypsum content as seen in the models.

The performances of MLR and MNLR were similar to each other for both calibration and validation stages. GRNN model performed excellently with R^2 value of 0.999 in the training stage. On the other hand, in the testing stage, its performance was comparable to that of the GA_based empirical model. It has to be noted that R^2 values of both GA_based empirical and GRNN models were higher than 0.90 for both stages.

For BFS pastes, the GRNN model was again the best one in the training (calibration) stage. Its R^2 was 0.981, and its errors were less than the errors of the other models (see Table 3). Different from the FA pastes, the performance of the MLR and GA_based empirical models was comparable to each other, and MNLR was the worst one during the calibration stage (see Table 3). On the other hand, for the validation stage, the GA_based empirical model yielded much less error than MNR and MNLR as was the case for FA pastes (see Tables 2, 3, and Fig. 6). The GRNN model performed similar to the GA_based empirical model in the validation (testing) stage. Similar to the FA pastes, the MLR and MNLR models predicted some strengths as negative values for the BFS pastes.

In addition to the work performed above, sensitivity analysis was also made as a further study. The GRNN model was selected for this purpose since it overall performed better than the others. In the sensitivity analysis, all of the 120
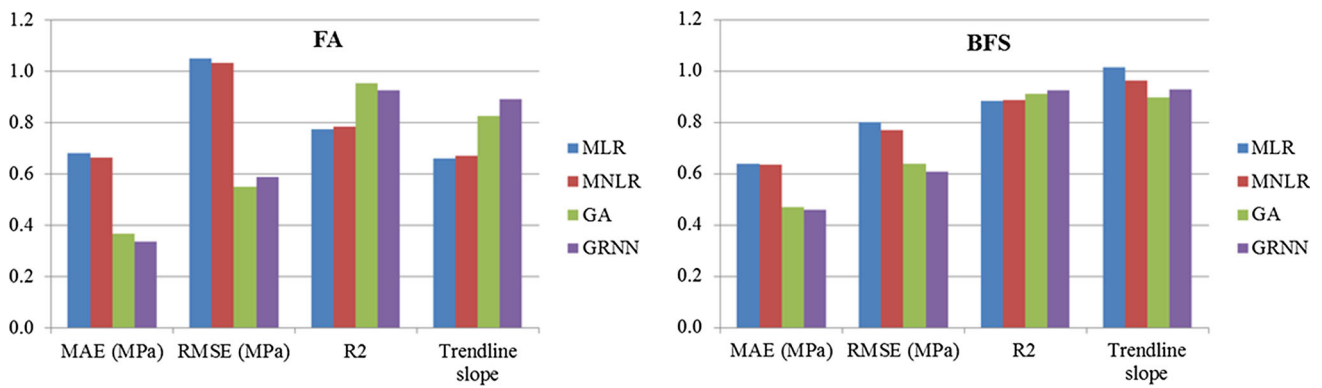
Fig. 6 Comparison of the performance of the models during the validation (testing) stage

Table 6 Sensitivity analysis for FA pastes

Parameters used	Excluded parameter	MAE (MPa)	RMSE (MPa)	R^2
G, FA, T, D, A	–	0.03	0.08	0.99
G, T, D, A	FA	0.03	0.07	0.99
G, FA, D, A	T	2.00	2.75	0.83
G, FA, T, A	D	1.43	1.8	0.11
G, FA, T, D	A	0.22	0.44	0.95

Table 7 Sensitivity analysis for BFS pastes

Parameters used	Excluded parameter	MAE (MPa)	RMSE (MPa)	R^2
G, BFS, T, D, A	–	0.52	0.64	0.92
G, T, D, A	BFS	0.53	0.64	0.91
G, BFS, D, A	T	0.66	0.82	0.86
G, BFS, T, A	D	1.52	1.87	0.27
G, BFS, T, D	A	0.66	0.83	0.81

datasets were used to predict the strength values. As a first step, all of the 5 input parameters (gypsum content, pozzolan content, curing temperature, curing duration and testing age) were included in the GRNN model. Predictions were made, and the MAE, RMSE, and R^2 values were calculated by comparing the actual and predicted data. Then, the analysis was repeated 4 times by excluding one of the parameters in each run. Accordingly, 1 analysis was made with 5 parameters and 4 analyses were made by 4 parameters. This procedure was performed for both FA and BFS pastes. The errors and the R^2 values for the sensitivity analysis are shown in Table 6 for FA and in Table 7 for BFS.

The sensitivity analysis results showed that for both FA and BFS pastes, R^2 values decreased significantly and the errors were relatively higher when the curing duration (D) is excluded in the prediction procedure (see Tables 6, 7). When the curing temperature (T) is not considered, the R^2 value was lower and the errors were higher especially for FA pastes (see Tables 6, 7). Therefore, for the further studies on the strength of gypsum pastes, it is recommended that the experimental program be designed to vary curing conditions

(temperature and duration) since their effect was more than that of the other parameters.

6 Summary and Conclusions

This study used the data on gypsum pastes containing several amounts of fly ash or ground granulated blast furnace slag (15, 30, 45, 60, and 75% of the pozzolan + gypsum mixture) which were cured at different temperatures (50 and 80 °C) for varying durations (4, 12, 24, and 72 h) and tested at 7, 14, and 28 days under compression to predict the strength of the gypsum pastes by multiple linear regression (MLR), multiple nonlinear regression (MNLR), and GA_based empirical, and GRNN models. Curing age, curing temperature, amount, and type of the additives can affect the strength of the gypsum pastes. To improve the strength of the gypsum pastes, trying all these parameters in an experimental study requires long time, much manpower, and high quantity of materials, resulting in a higher cost of the product. Therefore, mathematical

models can be very useful to predict the paste strength, which helps to reduce the number of trial batches.

Following conclusions are drawn from this study:

1. GRNN can be a useful tool for the prediction of strength. The input vector of the GRNN model is composed of gypsum content ($G\%$), pozzolan content (FA% or BFS%), curing temperature (T), curing duration (D), and testing age (Age).
2. The sensitivity analysis reveals that curing temperature (T) and especially curing duration (D) are important variables of the process. Therefore, this fact could be considered while designing an experimental program.
3. GA_based empirical models (Eqs. 12 and 13) accepting the same input vector as the GRNN model are found to be successful, and therefore, they can be applied for strength predictions.

$$\text{Strength} = 3 \times 10^{-5} * (G\%)^{0.0121} * (\text{FA}\%)^{0.3738}$$
$$* (T)^{1.3821} * (D)^{0.9824} * (\text{Age})^{0.182} \qquad (12)$$

$$\text{Strength} = 1 \times 10^{-4} * (G\%)^{0.2592} * (\text{BFS}\%)^{0.911}$$
$$* (T)^{0.7512} * (D)^{0.5985} * (\text{Age})^{0.3241} \qquad (13)$$

4. Although the MNLR model performed better than the MLR, its performance was poorer compared to those of the GRNN and the GA_based empirical models. MLR and MNLR models may not be proper ones for strength prediction. They can also produce implausible results.
5. The GRNN model can provide satisfactory estimates of strength, like the empirical models. However, due to the fact that neural networks are not good extrapolators, application of the GRNN model to another dataset would require retraining and retesting.
6. As opposed to the GRNN, the empirical models (Eqs. 12 and 13) are not fully black box models. They reveal, at least conceptually, the physics of the process by relating the gypsum content ($G\%$), pozzolan content (FA% or BFS%), curing temperature (T), curing duration (D), and testing age (age) to the strength.

To characterize the uncertain information more sufficiently and accurately, the future research can be in the direction of exploring Pythagorean fuzzy set which can serve as a foundation for developing more algorithms in decision making [32].

References

1. Crangle, R.D.: Gypsum, USGS 2015 minerals yearbook, pp. 33.1–33.10 (2015)
2. Çayırlı, H.: Alçıtaşı ve Türkiye Alçıtaşı Yatakları. Ulusal Alçı Kongresi Bildiriler Kitabı, 7–14, İstanbul (1991)
3. İstanbulluoğlu, Y.S.: A study on gypsum and anhydrite. Madencilik **36**(2), 13–23 (1997). **(in Turkish)**
4. Taylor, G.D.: Construction Materials, Longman Scientific and Technical. Longman Group UK Limited, Essex (1991)
5. Arıkan, M.; Sobolev, K.: The optimization of a gypsum-based composite material. Cem. Concr. Res. **32**(11), 1725–1728 (2002)
6. Singh, M.; Garg, M.: Phosphogypsum–fly ash cementitious binders – its hydration and strength development. Cem. Concr. Res. **25**(4), 752–758 (1995)
7. Çolak, A.: Physical, mechanical, and durability properties of gypsum–portland cement–natural pozzolan blends. Can. J. Civ. Eng. **28**(3), 375–382 (2001)
8. Cengiz, O.: Effects of pozzolan incorporation and curing conditions on strength and water resistance of natural gypsum pastes. Ph.D. Thesis, Middle East Technical University, Ankara, Turkey (2009).
9. Topcu, İ.B.; Sarıdemir, M.: Prediction of compressive strength of concrete containing fly ash using artificial neural networks and fuzzy logic. Comput. Mater. Sci. **41**(3), 305–311 (2008)
10. Hong-Guang, N.; Ji-Zong, W.: Prediction of compressive strength of concrete by neural networks. Cem. Concr. Res. **30**(8), 1245–1250 (2000)
11. Oztaş, A.; Pala, M.; Ozbay, E.; Kanca, E.; Cağlar, N.; Bhatti, M.A.: Predicting the compressive strength and slump of high strength concrete using neural network. Constr. Build. Mater. **20**(9), 769–775 (2006)
12. Yeh, I.-C.: Modeling of strength of high-performance concrete using artificial neural networks. Cem. Concr. Res. **28**(12), 1797–1808 (1998)
13. Dias, W.P.S.; Pooliyadda, S.P.: Neural networks for predicting properties of concretes with admixtures. Constr. Build. Mater. **15**(7), 371–379 (2001)
14. Erdem, T.K.; Tayfur, G.; Kırca, Ö.: Experimental and modeling study of strength of high strength concrete containing binary and ternary binders. Cem. Wapno Beton **16**(78), 224–237 (2011)
15. Oktay, B.M.; Odabaş, E.: Determining mechanical and physical properties of phospho-gypsum and perlite-admixtured plaster using an artificial neural network and regression models. Pol. J. Environ. Stud. **26**(5), 2425–2430 (2017)
16. Yılmaz, I.; Yüksek, G.: Prediction of the strength and elasticity modulus of gypsum using multiple regression, ANN, and ANFIS models. Int. J. Rock Mech. Min. Sci. **46**(4), 803–810 (2009)
17. Tayfur, G.: Soft Computing in Water Resources Engineering: Artifical Neural Networks, Fuzzy Logic and Genetic Algorithm. WIT Press, Southampton (2012)
18. Cigizoglu, H.K.; Alp, M.: Generalized regression neural network in modelling river sediment yield. Adv. Eng. Softw. **37**(2), 63–68 (2006)
19. Tsoukalas, L.H.; Uhrig, R.E.: Fuzzy and Neural Approaches in Engineering. Wiley, New York (1997)
20. Kim, S.; Shiri, J.; Kisi, O.; Singh, V.P.: Estimating daily pan evaporation using different data-driven methods and lag-time patterns. Water Resour. Manag. **27**(7), 2267–2286 (2013)
21. Cigizoglu, H.K.: Generalized regression neural network in monthly flow forecasting. Civ. Eng. Environ. Syst. **22**(2), 71–84 (2005)
22. Seckin, N.; Cobaner, M.; Yurtal, R.; Haktanir, T.: Comparison of artificial neural network methods with L-moments for estimating flood flow at ungauged sites: the case of East Mediterranean River basin, Turkey. Water Resour. Manag. **27**(7), 2103–2124 (2013)
23. Peng, X.; Dai, J.: A bibliometric analysis of neutrosophic set: two decades review from 1998–2017. Artif. Intell. Rev. (2018). https://doi.org/10.1007/s10462-018-9652-0
24. Peng, X.; Dai, J.: Approaches to single-valued neutrosophic MADM based on MABAC, TOPSIS and new similarity measure with score function. Neural Comput. Appl. **29**, 939–954 (2018)

25. Wang, L.; Sheng-Xiang Lv, S.-H.; Zeng, Y.-R.: Effective sparse adaboost method with ESN and FOA for industrial electricity consumption forecasting in China. Energy **155**, 1013–1031 (2018)
26. Wang, L.; Wang, Z.; Qu, H.; Liu, S.: Optimal forecast combination based on neural networks for time series forecasting. Appl. Soft Comput. **66**, 1–17 (2018)
27. Zeng, R.-Y.; Zeng, Y.; Choi, B.; Wang, L.: Multifactor-influenced energy consumption forecasting using enhanced back-propagation neural network. Energy **127**, 381–396 (2017)
28. Wang, L.; Hu, H.; Ai, X.-Y.; Liu, H.: Effective electricity energy consumption forecasting using echo state network improved by differential evolution algorithm. Energy **153**, 801–815 (2018)
29. Goldberg, D.E.: Genetic Algorithms for Search, Optimization, and Machine Learning. Addison-Wesley, USA (1989)
30. Sen, Z.: Genetic Algorithm and Optimization Methods. Turkish Water Foundation Publications, Istanbul (2004). **(in Turkish)**
31. Corporation, Palisade: Evolver, the Genetic Algorithm Solver for Microsoft Excel 2012. Newfield, New York (2012)
32. Peng, X.; Selvachandran, G.: Pythagorean fuzzy set: state of the art and future directions. Artif. Intell. Rev. **5**(3), 1873–1927 (2019)